


Review article

# Assessing Paleoclimate through Major and Trace Element Concentrations: A Review

Osama Shaltami<sup>1</sup> , Mustafa Ben Hkoma<sup>2</sup>

<sup>1</sup>Department of Earth Sciences, Faculty of Science, University of Benghazi, Libya

<sup>2</sup>Libyan Centre for Studies and Researches of Sciences and Environment Technology, Middle Zone Branch, Zliten, Libya

## ARTICLE INFO

Corresponding Email. [osama.rahil@yahoo.com](mailto:osama.rahil@yahoo.com)

Received: 12-08-2024

Accepted: 25-10-2024

Published: 09-11-2024

**Keywords.** Paleoclimate, Major Elements, Trace Elements.

**Copyright:** © 2024 by the authors. Submitted for possible open access publication under the terms and conditions of the Creative Commons Attribution International License (CC BY 4.0).

<http://creativecommons.org/licenses/by/4.0/>

## ABSTRACT

In geoscience, it is possible to deduce the paleoclimate of sediments from their lithology, fossil content, chemical composition, or geophysical characteristics. In this paper, the author reviewed the use of the concentration of major and trace elements to infer the paleoclimate. For this purpose, a variety of markers have been used in the previous studies, such as CIA, C.I, K<sub>2</sub>O/Al<sub>2</sub>O<sub>3</sub>, Al/Mg, Mg/Ca, Fe/Mn, Rb/Sr, Sr/Cu, Ga/Rb, Sr/Ba, ΣREE, and Eu anomaly. It should be noted that, for a more accurate evaluation of paleoclimate, discrimination diagrams (the plots of K<sub>2</sub>O+Na<sub>2</sub>O+Al<sub>2</sub>O<sub>3</sub> versus SiO<sub>2</sub>, CIA versus C.I, K<sub>2</sub>O/Al<sub>2</sub>O<sub>3</sub> versus Ga/Rb, Fe/Mn versus Sr/Ba, Rb/Sr versus Sr/Cu, and Mg/Ca-Al/Mg-ΣREE) are the recommended technique

**Cite this article.** Shaltami O, Ben Hkoma M. As-sessing Paleoclimate through Major and Trace Element Concentrations: A Review. *Alq J Med App Sci.* 2024;7(4):1187-1193. <https://doi.org/10.54361/ajmas.247440>

## INTRODUCTION

The climate of a former geological era is known as the paleoclimate. There are three distinct periods of paleoclimate that correspond to different geological ages: Precambrian, Phanerozoic, and Quaternary. Global paleoclimate markers are the proxies that are susceptible to changes in the global paleoclimatic condition. The majority of their origins are in marine sediments. Conversely, paleoclimate markers obtained from terrestrial sediments are frequently impacted by local tectonic shifts and paleogeographic fluctuations. Plate tectonics, which regulates the arrangement of continents, the interaction between the atmosphere and ocean, and the properties of Earth's orbit (Milankovitch cycles) are some of the factors that affect the climate system on Earth. Based on data gleaned from the examination of geologic materials global paleoclimate markers are developed. Generally, there are four types of paleoclimate markers: (1) Lithology [1-3]. (2) Fossil content [4-6]. (3) Chemical composition [7-9]. (4) Geophysical properties [10]. Elements and isotopes that record environmental data are among the geochemical markers [11,12]. Geochemists employ these markers to interpret paleoclimate environments. Concentrations of Si, Al, K, Na, Mg, Ca, Fe, Mn, Ga, Cr, Ni, V, Co, Sr, Ba, Cu, Rb, and REE can be used to determine paleoclimate [13-17]. In this work, the authors reviewed methods for evaluating paleoclimate based on the concentration of major and trace elements.

### Paleoclimate Markers

#### Chemical Index of Alteration

Numerous authors [e.g., 18 and 19] have extensively evaluated paleoclimatic conditions using the chemical index of alteration (CIA = (Al<sub>2</sub>O<sub>3</sub>/(Al<sub>2</sub>O<sub>3</sub>+CaO\*+Na<sub>2</sub>O+K<sub>2</sub>O))100, [20]). There are three methods to calculate the concentration of calcium oxide (CaO\*) in the silicate fraction:

(1)  $CaO^* = CaO - CO_{2(calcite)} - 0.5 \times CO_{2(dolomite)} - 10/3 \times P_2O_{5(apatite)}$  [21].

(2)  $CaO^* = CaO - P_2O_5$ , if  $Na_2O > CaO - P_2O_5$ , or  $CaO^* = Na_2O$ , if  $Na_2O < CaO - P_2O_5$  [22].

(3)  $CaO^* = CaO - SO_{3(anhydrite/gypsum)}$  [23].

Arid, semi-arid to semi-humid, and humid climates are characterized by CIA values of <70%, 70-80%, and 80-100%, correspondingly [20]. [24] pointed out the limitations of the CIA, despite its usefulness in interpreting paleoclimatic conditions. They believed that the existence of carbonate-rich sediments, post-depositional potassium addition, and the hereditary of clays from the source area could restrict the reliance on the CIA as a paleoclimate parameter. They suggested that the CIA is a valuable resource for determining paleoclimate conditions, if used with the proper caution. In order to estimate climate changes, [25] demonstrated a positive correlation between land surface temperatures and CIA on a global scale. The surface temperature can be ascertained using the following equation:  $T(^{\circ}\text{C}) = 0.56 \times \text{CIA} - 25.7$  [26]. The correlation held true with an uncertainty of approximately  $\pm 5^{\circ}\text{C}$  when CIA and T ranged from ~50 to 90% and ~3 to 25  $^{\circ}\text{C}$ , correspondingly [26]. A correlation between CIA and mean annual precipitation (MAP) without K (CIA-K) was suggested by [27]:  $\text{MAP}^{\text{CIA-K}} = 221e^{0.0197(\text{CIA-K})}$ . This correlation was modified by [28] as follows:  $\text{MAP}^{\text{CIA}} = 169e^{0.0271(\text{CIA})}$ .

### ***Climatic Index***

The climatic index (C.I = (Fe+Mn+Cr+Ni+V+Co)/(Ca+Mg+Sr+Ba+K+Na), [15]) is utilized as a paleoclimate reference. C.I also referred to as C-value. The underlying suggestion for C.I is that, there is an increase in Fe, Mn, Cr, Ni, V, and Co in humid environments; while in arid environments, saline minerals precipitate as water alkalinity increases due to evaporation, resulting in the enrichment of Ca, Mg, K, Na, Sr, and Ba [7 and 15]. Humid, semi-humid, semi-arid to semi-humid, semi-arid, and arid climates are represented by C.I values of >0.8, 0.6-0.8, 0.4-0.6, 0.2-0.4, and <0.2, respectively [8 and 29].

### ***K<sub>2</sub>O/Al<sub>2</sub>O<sub>3</sub> Ratio***

Feldspars and clay minerals can be distinguished using the K<sub>2</sub>O/Al<sub>2</sub>O<sub>3</sub> ratio. Feldspars have a higher ratio (0.3-0.9) compared to clay minerals (0-0.3, [30]). Furthermore, the ratio in illite (0.2-0.3, [31]) is higher than that in kaolinite, smectite, and vermiculite (nearly zero, [30]). Accordingly, humid conditions are characterized by low K<sub>2</sub>O/Al<sub>2</sub>O<sub>3</sub> ratios (<0.2), while the ratios are high in arid climates (>0.2, [32]).

### ***Fe/Mn Ratio***

The Fe/Mn ratio can be used to provide paleoclimatic evidence [33 and 34]. Mn concentration is low in humid conditions where Fe is rapidly precipitated from colloidal iron hydroxides, whereas Mn content is typically high in arid climates. Therefore, humid climates are linked to high Fe/Mn ratios (>1), whereas arid environments are characterized by low ratios (<1) [33].

### ***Al/Mg Ratio***

The Al/Mg ratio can reveal information about the paleoclimate during deposition; low ratios suggest an arid environment, while high ratios indicate a humid climate [33].

### ***Mg/Ca Ratio***

The Mg/Ca ratio is frequently used as a paleoclimate proxy in clastic rocks [33 and 35]. High ratios are generally indicative of arid climates, whereas low ratios are characteristically reflective of humid climates [33].

### ***Rb/Sr Ratio***

The Rb/Sr ratio is a significant index of paleoclimate [36]. During weathering, Sr is depleted through leaching, whereas Rb remains relatively stable. Sr is depleted and the Rb/Sr ratio rises (>0.5) as a result of increased precipitation and increased weathering in humid climates. Since there is less precipitation, less weathering, and more Sr-rich rocks in arid climates, the Rb/Sr ratio would be relatively low (<0.5) [36].

### ***Sr/Cu Ratio***

Paleoclimate studies have used the Sr/Cu ratio as a reliable indicator [37]. Similar to Rb, Cu does not change during weathering. The typical Sr/Cu ratios for humid, semi-arid to semi-humid, and arid climates are 1.3-5, 5-10, and >10, correspondingly [37].

### ***Ga/Rb ratio***

The paleoclimate system is often constrained by the Ga/Rb ratio [32]. In general, Ga is more abundant in kaolinite, suggesting humid conditions, whereas Rb is more commonly found in illite, signifying an arid environment [38]. Consequently, the Ga/Rb ratio is high in humid conditions (>0.21), while arid climates show low ratios (<0.21) [32].

### Sr/Ba Ratio

Paleoclimate can be assessed based on the Sr/Ba ratio [34 and 39]. Climate has an impact on the Sr/Ba ratio; high ratios (>1) represent arid conditions, while low ratios (<1) indicate humid climates [39].

### Rare Earth Elements

REE are very sensitive to variations in the paleoclimate [40-42]. The most important parameters are  $\Sigma$ REE [42] and Eu anomaly [40]. Eu anomaly can be calculated using the following equation:  $Eu_{found}/Eu^*_{expected} = Eu_N / (Sm_N \times Gd_N)^{0.5}$ . The REE values used in this equation are shale normalized. For normalization, the Post Archean Australian Shale (PAAS, [43]) and the North American Shale Composite (NASC, [44]) are utilized. Generally, humid climates display high  $\Sigma$ REE [42] and large negative Eu anomaly [40]. According to [41], weak weathering of REE-bearing minerals would result in weak secondary LREE-carrying product development and a drop in the (La/Yb)<sub>N</sub> ratio.

### Discrimination Diagrams

Discrimination diagrams are the preferred method for more accurate paleoclimate evaluation. There are many discrimination diagrams that depend on the paleoclimate markers, such as the binary plots of K<sub>2</sub>O+Na<sub>2</sub>O+Al<sub>2</sub>O<sub>3</sub> versus SiO<sub>2</sub> (Fig. 1), CIA versus C.I (Fig. 2), K<sub>2</sub>O/Al<sub>2</sub>O<sub>3</sub> versus Ga/Rb (Fig. 3), Fe/Mn versus Sr/Ba (Fig. 4), and Rb/Sr versus Sr/Cu (Fig. 5), and the triplot of Mg/Ca-Al/Mg- $\Sigma$ REE (Fig. 6).

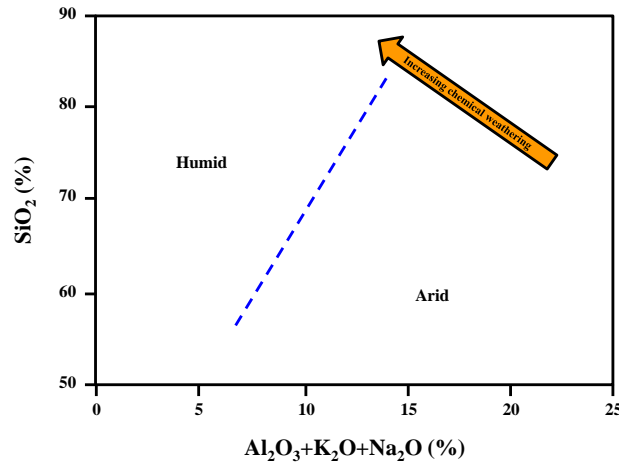


**Figure 1. Binary plot of CIA vs. C.I [after 8, 20, and 29].**

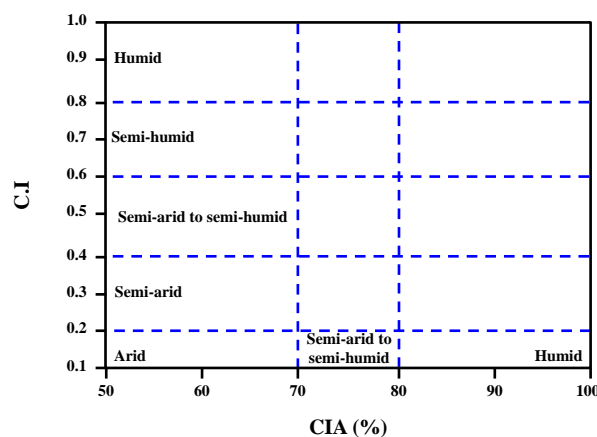


**Figure 2. Binary plot of CIA vs. C.I [after 8, 20, and 29].**

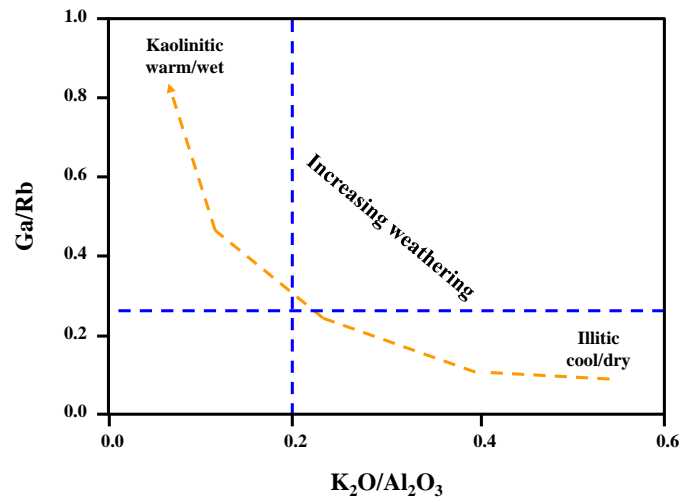


Figure 3. Binary plot of  $K_2O/Al_2O_3$  vs.  $Ga/Rb$  [32].

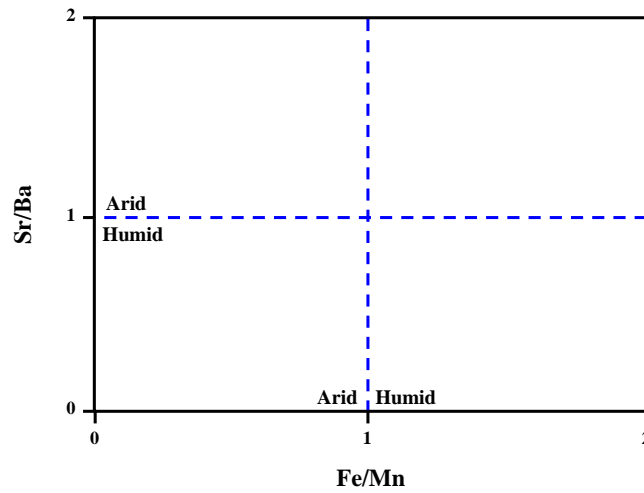


Figure 4. Binary plot of  $Fe/Mn$  vs.  $Sr/Ba$  [after 33 and 39].

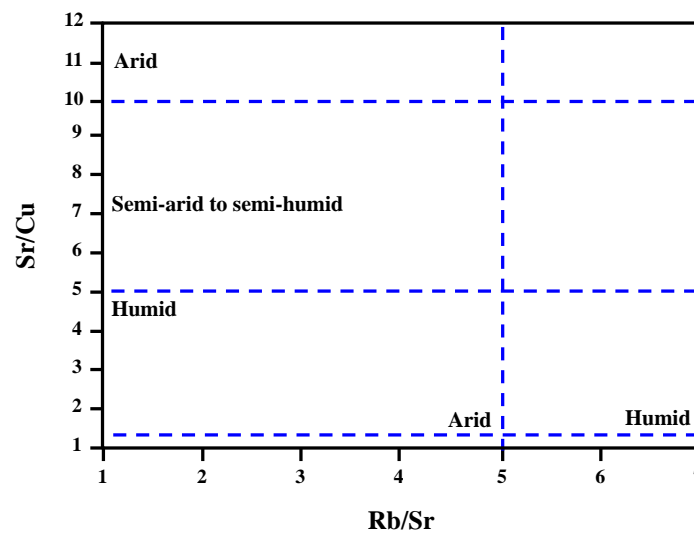


Figure 5. Binary plot of  $Rb/Sr$  vs.  $Sr/Cu$  [after 36 and 37].

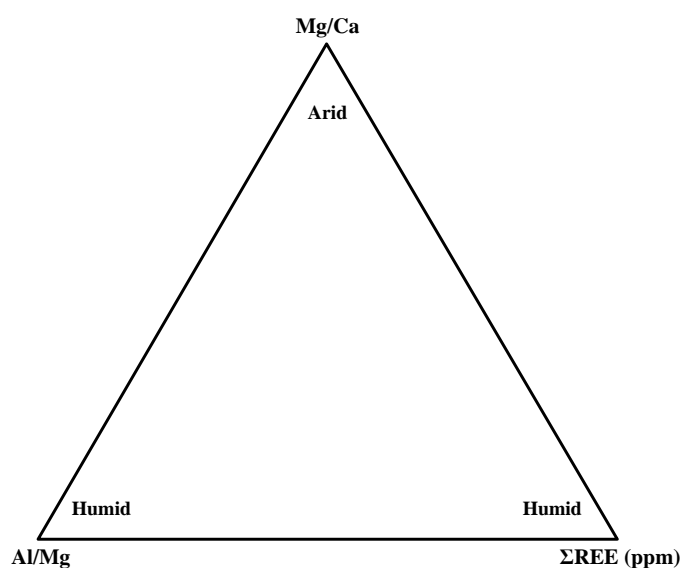


Figure 6. Triplot of Mg/Ca-Al/Mg-ΣREE [after 33 and 42].

## CONCLUSION

Two conclusions can be drawn from this work: (1) Numerous markers, including CIA, C.I,  $K_2O/Al_2O_3$ , Al/Mg, Mg/Ca, Fe/Mn, Rb/Sr, Sr/Cu, Ga/Rb, Sr/Ba, ΣREE, and Eu anomaly, can be used to determine the paleoclimate of sediments. (2) The best approach for a more precise assessment of paleoclimate is to use discrimination diagrams such as the plots of  $K_2O+Na_2O+Al_2O_3$  versus  $SiO_2$ , CIA versus C.I,  $K_2O/Al_2O_3$  versus Ga/Rb, Fe/Mn versus Sr/Ba, Rb/Sr versus Sr/Cu, and Mg/Ca- Al/Mg-ΣREE.

## REFERENCES

- Noble PJ, Ball GI, Zimmerman SH, Maloney J, Smith SB, Kent G, Adams KD, Karlin RE, Driscoll N. Holocene paleoclimate history of Fallen Leaf Lake, CA., from geochemistry and sedimentology of well-dated sediment cores. *Quaternary Science Reviews*. 2016 Jan 1;131:193-210.
- Fedorchuk ND, Isbell JL, Griffis NP, Vesely FF, Rosa EL, Montañez IP, Mundil R, Yin QZ, Iannuzzi R, Roesler G, Pauls KN. Carboniferous glaciotectionized sediments in the southernmost Paraná Basin, Brazil: Ice marginal dynamics and paleoclimate indicators. *Sedimentary geology*. 2019 Jul 1;389:54-72.
- Gao Y, Tian Z, Qu X, Wang G, Wang P, Zhang S, Tang H. Paleoclimatic and Paleogeographic Significance of the Early Santonian Ice-Rafted Dropstones in the Songliao Basin, Ne China. *Ne China*.
- Luoto TP, Nevalainen L, Kauppila T, Tammelin M, Sarmaja-Korjonen K. Diatom-inferred total phosphorus from dystrophic Lake Arapisto, Finland, in relation to Holocene paleoclimate. *Quaternary Research*. 2012 Sep;78(2):248-55.
- Kim Y, Yi S, Kim GY, Lee E, Kong S. Palynological study of paleoclimate and paleoceanographic changes in the Eastern South Korea Plateau, East Sea, during the Plio-Pleistocene climate transition. *Palaeogeography, Palaeoclimatology, Palaeoecology*. 2019 Apr 15;520:18-29.
- Korasidis VA, Wallace MW, Chang TJ, Phillips D. Eocene paleoclimate and young mountain-building in the Australian Eastern Highlands. *Review of Palaeobotany and Palynology*. 2023 May 1;312:104875.
- Tao S, Xu Y, Tang D, Xu H, Li S, Chen S, Liu W, Cui Y, Gou M. Geochemistry of the Shitoumei oil shale in the Santanghu Basin, Northwest China: Implications for paleoclimate conditions, weathering, provenance and tectonic setting. *International Journal of Coal Geology*. 2017 Nov 1;184:42-56.
- Awan RS, Liu C, Gong H, Dun C, Tong C, Chamssidini LG. Paleo-sedimentary environment in relation to enrichment of organic matter of Early Cambrian black rocks of Niutitang Formation from Xiangxi area China. *Marine and Petroleum Geology*. 2020 Feb 1;112:104057.
- Shaltami OR. Elemental geochemistry of the Awainat Wanin Formation in three selected areas, Murzuq Basin, SW Libya. *GSI*. 2024 Feb;12(2).
- Peng C, Zou C, Zhang S, Shu J, Wang C. Geophysical logs as proxies for cyclostratigraphy: Sensitivity evaluation, proxy selection, and paleoclimatic interpretation. *Earth-Science Reviews*. 2024 Mar 7:104735.
- Zhang X, Gao Z, Fan T, Xue J, Li W, Zhang H, Cao F. Element geochemical characteristics, provenance attributes, and paleosedimentary environment of the Paleogene strata in the Lenghu area, northwestern Qaidam Basin. *Journal of Petroleum Science and Engineering*. 2020 Dec 1;195:107750.

12. Platt BF, Smith JJ. Late Miocene paleoecology and paleoclimate in the central High Plains of North America reconstructed from paleopedological, ichnological, and stable isotope analyses of the Ogallala Formation in western Kansas, USA. *Evolving Earth*. 2023 Dec 1;1:100019.
13. Suttner LJ, Dutta PK. Alluvial sandstone composition and paleoclimate; I, Framework mineralogy. *Journal of Sedimentary Research*. 1986 May 1;56(3):329-45.
14. Beckmann B, Flögel S, Hofmann P, Schulz M, Wagner T. Orbital forcing of Cretaceous river discharge in tropical Africa and ocean response. *Nature*. 2005 Sep 8;437(7056):241-4.
15. Cao J, Wu M, Chen Y, Hu K, Bian L, Wang L, Zhang Y. Trace and rare earth element geochemistry of Jurassic mudstones in the northern Qaidam Basin, northwest China. *Geochemistry*. 2012 Sep 1;72(3):245-52.
16. Zhang L, Dong D, Qiu Z, Wu C, Zhang Q, Wang Y, Liu D, Deng Z, Zhou S, Pan S. Sedimentology and geochemistry of Carboniferous-Permian marine-continental transitional shales in the eastern Ordos Basin, North China. *Palaeogeography, Palaeoclimatology, Palaeoecology*. 2021 Jun 1;571:110389.
17. Xiao B, Guo D, Li S, Xiong S, Jing Z, Feng M, Fu X, Zhao Z. Rare Earth Element Characteristics of Shales from Wufeng–Longmaxi Formations in Deep-Buried Areas of the Northern Sichuan Basin, Southern China: Implications for Provenance, Depositional Conditions, and Paleoclimate. *ACS omega*. 2024 Jan 1;9(2):2088-103.
18. El Mourabet M, Barakat A, Zaghoul MN, El Baghdadi M. Geochemistry of the Miocene Zoumi flysch thrust-top basin (External Rif, Morocco): new constraints on source area weathering, recycling processes, and paleoclimate conditions. *Arabian Journal of Geosciences*. 2018 Mar;11:1-20.
19. Khan D, Zijun L, Qiu L, Kuiyuan L, Yongqiang Y, Cong N, Bin L, Li X, Habulashenmu Y. Mineralogical and geochemical characterization of lacustrine calcareous shale in Dongying Depression, Bohai Bay Basin: Implications for paleosalinity, paleoclimate, and paleoredox conditions. *Geochemistry*. 2023 Sep 1;83(3):125978.
20. Nesbitt H, Young GM. Early Proterozoic climates and plate motions inferred from major element chemistry of lutites. *nature*. 1982 Oct 21;299(5885):715-7.
21. Fedo CM, Wayne Nesbitt H, Young GM. Unraveling the effects of potassium metasomatism in sedimentary rocks and paleosols, with implications for paleoweathering conditions and provenance. *Geology*. 1995 Oct 1;23(10):921-4.
22. McLennan SM, Hemming S, McDaniel DK, Hanson GN. Geochemical approaches to sedimentation, provenance, and tectonics.
23. Scheibe, C. (2021): Chemical index of alteration (available at <https://chemostratigraphy.com/chemical-index-of-alteration-nesbitt-young-1982/>).
24. Goldberg K, Humayun M. The applicability of the Chemical Index of Alteration as a paleoclimatic indicator: An example from the Permian of the Paraná Basin, Brazil. *Palaeogeography, Palaeoclimatology, Palaeoecology*. 2010 Jul 1;293(1-2):175-83.
25. Yang J, Cawood PA, Du Y, Feng B, Yan J. Global continental weathering trends across the Early Permian glacial to postglacial transition: Correlating high-and low-paleolatitude sedimentary records. *Geology*. 2014 Oct 1;42(10):835-8.
26. Cao Y, Song H, Algeo TJ, Chu D, Du Y, Tian L, Wang Y, Tong J. Intensified chemical weathering during the Permian-Triassic transition recorded in terrestrial and marine successions. *Palaeogeography, Palaeoclimatology, Palaeoecology*. 2019 Apr 1;519:166-77.
27. Sheldon ND, Retallack GJ, Tanaka S. Geochemical climofunctions from North American soils and application to paleosols across the Eocene-Oligocene boundary in Oregon. *The Journal of geology*. 2002 Nov;110(6):687-96.
28. Perri F. Chemical weathering of crystalline rocks in contrasting climatic conditions using geochemical proxies: an overview. *Palaeogeography, Palaeoclimatology, Palaeoecology*. 2020 Oct 15;556:109873.
29. Ding J, Zhang J, Tang X, Huo Z, Han S, Lang Y, Zheng Y, Li X, Liu T. Elemental geochemical evidence for depositional conditions and organic matter enrichment of black rock series strata in an inter-platform basin: The Lower Carboniferous Datang Formation, Southern Guizhou, Southwest China. *Minerals*. 2018 Nov 6;8(11):509.
30. Cox R, Lowe DR, Cullers RL. The influence of sediment recycling and basement composition on evolution of mudrock chemistry in the southwestern United States. *Geochimica et Cosmochimica Acta*. 1995 Jul 1;59(14):2919-40.
31. Zhou JX, Bai JH, Huang ZL, Zhu D, Yan ZF, Lv ZC. Geology, isotope geochemistry and geochronology of the Jinshachang carbonate-hosted Pb–Zn deposit, southwest China. *Journal of Asian Earth Sciences*. 2015 Feb 1;98:272-84.
32. Roy DK, Roser BP. Climatic control on the composition of Carboniferous–Permian Gondwana sediments, Khalaspir basin, Bangladesh. *Gondwana Research*. 2013 Apr 1;23(3):1163-71.
33. Yan K, Wang CL, Mischke S, Wang JY, Shen LJ, Yu XC, Meng LY. Major and trace-element geochemistry of Late Cretaceous clastic rocks in the Jitai Basin, southeast China. *Scientific Reports*. 2021 Jul 5;11(1):13846.
34. Eric BE, Adama A, Etutu ME, Kwankam FN, Betrant BS, Esue MF. Paleoclimate characteristics of source area weathering and metallogenic implication of cretaceous black shales in the Mamfe basin,(SW Cameroon): Evidence from litho-geochemistry. *Heliyon*. 2023 Jun 1;9(6).
35. Deng T, Li Y, Wang Z, Yu Q, Dong S, Yan L, Hu W, Chen B. Geochemical characteristics and organic matter enrichment mechanism of black shale in the Upper Triassic Xujiahe Formation in the Sichuan basin: Implications for paleoweathering, provenance and tectonic setting. *Marine and Petroleum Geology*. 2019 Nov 1;109:698-716.



36. Zou C, Mao L, Tan Z, Zhou L, Liu L. Geochemistry of major and trace elements in sediments from the Lubei Plain, China: Constraints for paleoclimate, paleosalinity, and paleoredox environment. *Journal of Asian Earth Sciences*: X. 2021 Dec 1;6:100071.
37. Lerman A. *Lakes: chemistry, geology, physics*. 1978.
38. Roy DK, Roser BP. Geochemical evolution of the Tertiary succession of the NW shelf, Bengal basin, Bangladesh: Implications for provenance, paleoweathering and Himalayan erosion. *Journal of Asian Earth Sciences*. 2013 Dec 15;78:248-62.
39. Dai S, Bechtel A, Eble CF, Flores RM, French D, Graham IT, Hood MM, Hower JC, Korasidis VA, Moore TA, Püttmann W. Recognition of peat depositional environments in coal: A review. *International Journal of Coal Geology*. 2020 Feb 15;219:103383.
40. Condie KC. Another look at rare earth elements in shales. *Geochimica et Cosmochimica Acta*. 1991 Sep 1;55(9):2527-31.
41. Yang Y, Fang X, Galy A, Li M, Appel E, Liu X. Paleoclimatic significance of rare earth element record of the calcareous lacustrine sediments from a long core (SG-1) in the western Qaidam Basin, NE Tibetan Plateau. *Journal of Geochemical Exploration*. 2014 Oct 1;145:223-32.
42. Ma FH, Zhang Y, Pan JL, Wu WZ. Geochemical characteristics of rare earth element and their geological significance of mud-shale in Cretaceous Madongshan Formation, Liupanshan Basin. *Geological Review*. 2021;67(1):209-17.
43. Taylor SR. *The continental crust: Its composition and evolution*. Geoscience Texts. 1985;312.
44. Gromet LP, Haskin LA, Korotev RL, Dymek RF. The "North American shale composite": Its compilation, major and trace element characteristics. *Geochimica et cosmochimica acta*. 1984 Dec 1;48(12):2469-82.

## تقييم المناخ القديم من خلال تركيزات العناصر الرئيسية والعناصر النزرة: مراجعة

أسامة الشلطي<sup>1\*</sup>، مصطفى بن حكومة<sup>2</sup>

<sup>1</sup>قسم علوم الأرض، كلية العلوم، جامعة بنغازي، ليبيا

<sup>2</sup>المركز الليبي للدراسات والبحوث في العلوم وتكنولوجيا البيئة، فرع المنطقة الوسطى، زليتن، ليبيا

### المخلص

في علم الأرض، من الممكن استنتاج المناخ القديم للرواسب من خلال خصائصها الصخرية أو محتواها الأحفوري أو تركيبها الكيميائي أو خصائصها الجيوفيزيائية. في هذه الورقة، استعرض المؤلف استخدام تركيز العناصر الرئيسية والعناصر النزرة لاستنتاج المناخ القديم. لهذا الغرض، تم استخدام مجموعة متنوعة من العلامات في الدراسات السابقة، مثل CIA و C.I و K<sub>2</sub>O/Al<sub>2</sub>O<sub>3</sub> و Al/Mg و Mg/Ca و Fe/Mn و Rb/Sr و Sr/Cu و Ga/Rb و Sr/Ba و ΣREE وشذوذ Eu. تجدر الإشارة إلى أنه من أجل تقييم أكثر دقة للمناخ القديم، فإن مخططات التمييز مخططات K<sub>2</sub>O+Na<sub>2</sub>O+Al<sub>2</sub>O<sub>3</sub> مقابل SiO<sub>2</sub>، و CIA مقابل C.I، و K<sub>2</sub>O/Al<sub>2</sub>O<sub>3</sub> مقابل Ga/Rb، و Fe/Mn مقابل Sr/Ba، و Rb/Sr مقابل Sr/Cu، و (Mg/Ca-Al/Mg-ΣREE) هي التقنية الموصى بها الكلمات المفتاحية. المناخ القديم، العناصر الرئيسية، العناصر النزرة.